Excitons in large-gap insulators: Solid argon*

W. Andreoni
Istituto di Fisica, Università di Roma, Roma, Italy

M. Altarelli
Department of Physics, University of Illinois at Urbana-Champaign, Urbana, Illinois 61801

F. Bassani
Istituto di Fisica, Università di Roma, Roma, Italy

(Received 30 September 1974)

The theory of excitons for the range intermediate between the Frenkel-Peierls and the Wannier-Mott models is formulated in terms of the band structure $E_n(\vec{k})$ and the Coulomb and exchange integrals involving the Wannier functions of the valence and conduction bands. When the band structure is that appropriate to solid rare gases and alkali halides, the problem simplifies greatly if the electron and the hole can be assumed to be confined to the same unit cell. Taking full account of the symmetry, the problem in this case reduces to the diagonalization of a simple second-order Fredholm determinant. Numerical calculations are performed for the lowest transverse and longitudinal exciton states of solid argon. The Wannier function for the valence bands is replaced by the $3p$ atomic orbitals, and that for the conduction band is computed by approximating the Bloch functions with an orthogonalized plane wave. Very good agreement with experimental results is obtained for the lowest exciton doublet. The doublet splitting and the relative intensities of the two peaks are computed in terms of the ratio of the exchange integrals to the spin-orbit splitting of the valence bands. The conclusions are extended to the other solid rare gases.

I. INTRODUCTION

Exciton states have been investigated by solid-state theorists for a long time,[1] and excitonic spectra have been observed experimentally in a large number of materials.[2] From the theoretical point of view, the Wannier-Mott picture, based on the effective-mass approximation, has been most successful in describing weakly bound excitons in semiconductors with a high dielectric constant. The agreement with experiment has been improved by including effects due to anisotropy,[3] band degeneracies,[4] and central-cell corrections[5] in this theory. The Frenkel-Peierls model, on the other hand, is appropriate to tightly bound excitons, and has proven useful for molecular crystals.[6]

In the region of intermediate binding, which covers the lowest exciton states of most compounds and all large-gap insulators, one must take into account the structure of the valence and conduction bands throughout the Brillouin zone. To this aim, an approach based on the integral-equation formalism has been suggested recently,[7] and preliminary calculations performed for solid argon provided encouraging results.[8]

The solid rare gases constitute indeed an ideal test ground for theories of intermediately bound excitons. The excitonic spectrum has been investigated experimentally in great detail, by optical[9] and electron energy-loss[10] techniques, and the observed structure can be qualitatively ascribed to two Rydberg series separated by the valence-band spin-orbit splitting.[9,10] There was an attempt by Knox[11] to apply the Frenkel-Peierls model to solid argon, but because of the large overlap of the $4s$ atomic functions this approach proved inadequate. On the other hand, although the classification of exciton lines has often been made according to the effective-mass scheme, this approximation failed to produce quantitative agreement.[9] Hermanson[5] attributed the discrepancy to the presence of central-cell corrections in the electron-hole interaction and computed their effect by pseudopotential theory. Rössler and Schutz[12] improved these calculations, and extended them to solid argon. Their results for the lowest excitons are in good agreement with experiment. However, it should be noticed that the calculation of the screened exciton pseudopotential (and of its matrix elements between oversimplified Wannier functions) is very schematic. Furthermore, the neglect of the spin-orbit splitting of the valence bands and of their exchange-induced mixing, which has a large effect on the ground-state wave function (as discussed in Sec. V is not justified and cannot account for the doublet nature of the lowest exciton lines and their relative intensities.

It is the purpose of the present paper to extend the integral-equation method which we presented in Refs. 7 and 8 and to apply it to the fundamental absorption edge of solid argon. The key approximation is to assume that the electron and the hole are confined to the same unit cell, as suggested by

the fact that the Bohr radii of the $n=1$ excitons[12] are smaller than the nearest-neighbor distance.

It is then possible to solve the integral equation for the exciton eigenvalues and eigenstates very easily and without adjustable parameters. The input of the calculation is a knowledge of the band-structure features and of the properties of the conduction and valence Bloch functions. It is shown that the energies of the exciton states depend on integrated quantities such as the Green's function $G_{n,n'}(E)$ and the Wannier functions $a_n(\vec{r})$, and they are not very sensitive to the details of the band structure. The Wannier function for the conduction band is computed by assuming that a single orthogonalized plane wave contains the salient features of the conduction Bloch functions. The Green's function is computed by interpolating the band structure with a three-term tight-binding formula, the parameters being determined by the effective mass at Γ and the band energy at X and L. Since we now consider explicitly the nonspherical components of the conduction Wannier function in the computation of Coulomb and exchange integrals, and we use an accurate description of the entire band structure in the Green's function, we obtain good agreement with experiment for the position of the exciton doublet, for the splitting, and for the relative intensities of its two components. The latter two quantities are shown to be strictly dependent on the ratio of the exchange energy to the spin-orbit splitting of the valence band, and this allows an interpretation of the doublet separation and intensities in the whole family of solid rare gases.

The results obtained will allow us to conclude that the integral-equation approach is a viable *ab initio* procedure for the computation of exciton states in the intermediate-binding regime.

In Sec. II we briefly recall the general method and discuss the approximation to one cell of the crystal. In Sec. III we derive the simplified equations for the optically relevant exciton states in the case of the specific band structure of solid rare gases and alkali halides and in the one-site approximation. In Sec. IV the computation of the Green's function, of the Wannier functions, and of the Coulomb and exchange integrals occurring in the eigenvalue equation is described. In Sec. V the lowest exciton states of solid argon are obtained and the dependence of the results on the details of the band structure and on the value of the exchange integral is discussed. Finally, in Sec. VI we compare the results to experiment, draw some conclusions, and sketch lines of future progress.

II. GENERAL FORMULATION AND ONE-SITE APPROXIMATION

We now briefly summarize the procedure of calculation of exciton energies and wave functions in the case of intermediate binding. The procedure has been described in Refs. 7 and 8 and has been termed the "integral-equation method" because it attacks the basic integral equation of the exciton problem. The method is very similar to the Green's-function approach of Takeuti[13] but it allows a better analysis of the relevant approximations and is extended more naturally to the case of degenerate bands.

We start by expanding the exciton state $|\Psi_{\vec{q}}\rangle$, with crystal momentum $\vec{q}$, in the basis of Slater determinants with an electron shifted from the valence band state $|v\vec{k}\rangle$ to the conduction state $|c\vec{k}+\vec{q}\rangle$,

$$|\Psi_{\vec{q}}\rangle = \sum_{cv}\sum_{\vec{k}} A_{cv}(\vec{k})\,|v\vec{k}, c\vec{k}+\vec{q}\rangle \quad , \tag{1}$$

where the ket on the right-hand side denotes the Slater determinant, and the indices c and v contain the spin functions. The Schrödinger equation yields the following integral equation for the expansion coefficients $A_{cv}(\vec{k})$:

$$[E_c(\vec{k}+\vec{q}) - E_v(\vec{k}) - E]A_{cv}(\vec{k}) + \sum_{c'v'}\sum_{\vec{k}'} A_{c'v'}(\vec{k}') \times U_{cv,c'v'}(\vec{k},\vec{k}',\vec{q}) = 0 \ , \tag{2a}$$

where the kernels are

$$\begin{aligned} U_{cv,c'v'}(\vec{k},\vec{k}',\vec{q}) = &-\int\int d\tau_1 d\tau_2\, \Psi_c^*(\vec{k}+\vec{q},\tau_1)\Psi_{v'}^*(\vec{k}',\tau^2) \\ &\times \frac{e^2}{r_{12}}\Psi_{c'}(\vec{k}'+\vec{q},\tau_1)\,\Psi_v(\vec{k},\tau_2) \\ &+\int\int d\tau_1 d\tau_2\, \Psi_c^*(\vec{k}+\vec{q},\tau_1)\,\Psi_{v'}^*(\vec{k}',\tau_2) \\ &\times \frac{e^2}{r_{12}}\Psi_{c'}(\vec{k}'+\vec{q},\tau_2)\,\Psi_v(\vec{k},\tau_1) \end{aligned} \tag{2b}$$

and the integrations include summation over the spin variables.

The symmetry of the exciton states can be imposed from the beginning by choosing appropriate combinations of Slater determinants which have the full symmetry of the wave vector $\vec{q}$. The kernels will then involve combinations of terms of the type (2b); in each of them the sum on the spin variables can be immediately performed and we are left with combinations of space integrals. When spin-orbit effects are considered, the total spin part cannot be separated from the total space part, and we do not have two separate kernels for singlet and triplet states, but $S=0$ and $S=1$ are mixed.

It is important to point out that screening effects are not included in Eq. (2). One can introduce an appropriate screening function according to the prescriptions of several authors.[14] This corresponds to replacing e^2/r_{12} with $g(r_{12})=e^2/\epsilon(r_{12})r_{12}$ in the denominators of Eq. (2b), where the function $\epsilon(r_{12})$

varies between 1, when $r_{12} \to 0$, and ϵ_0, the static dielectric constant of the crystal, for large r_{12}.

In order to solve Eq. (2a), it is most convenient to expand the Bloch functions appearing in Eq. (2b) in terms of the Wannier functions localized on the lattice points $\vec{R}$,

$$a_i(\vec{r}-\vec{R}) = N^{-1/2} \sum_{\vec{k}} \Psi_i(\vec{k},\vec{r}) e^{-i\vec{k}\cdot\vec{R}} \quad . \tag{3}$$

The kernel is then written

$$U_{cv,c'v'}(\vec{k},\vec{k}',\vec{q}) = \frac{1}{N} \sum_{\vec{R},\vec{R}',\vec{R}''} e^{-i\vec{q}\cdot(\vec{R}-\vec{R}')} \left(\delta_{\sigma_c\sigma_{c'}} \delta_{\sigma_v\sigma_{v'}} \int\int d\vec{r}_1 d\vec{r}_2 a_c^*(\vec{r}_1-\vec{R}) a_{v'}^*(\vec{r}_2-\vec{R}'') g(r_{12}) a_{c'}(\vec{r}_1-\vec{R}') a_v(\vec{r}_2) \right.$$
$$\left. + \delta_{\sigma_c\sigma_v} \delta_{\sigma_{c'}\sigma_{v'}} \int\int d\vec{r}_1 d\vec{r}_2 a_c^*(\vec{r}_1-\vec{R}) a_{v'}^*(\vec{r}_2-\vec{R}'') g(r_{12}) a_{c'}(\vec{r}_2-\vec{R}') a_v(\vec{r}_1) \right) e^{-i\vec{k}\cdot\vec{R}} e^{i\vec{k}'\cdot(\vec{R}'-\vec{R}'')} \quad . \tag{4}$$

On the basis of arguments discussed in detail by Horie,[15] we retain only the dominant contributions to Eq. (4), namely, the following Coulomb and exchange integrals:

$$Q(\vec{R}) = \int\int d\vec{r}_1 d\vec{r}_2 a_c^*(\vec{r}_1-\vec{R}) a_{v'}^*(\vec{r}_2) g(r_{12}) \times a_{c'}(\vec{r}_1-\vec{R}) a_v(\vec{r}_2) \quad , \tag{5}$$

$$J_1(\vec{R}) = \int\int d\vec{r}_1 d\vec{r}_2 a_c^*(\vec{r}_1) \times a_{v'}^*(\vec{r}_2-\vec{R}) g(r_{12}) a_{c'}(\vec{r}_2-\vec{R}) a_v(\vec{r}_1) \quad , \tag{6}$$

$$J_2(\vec{R}) = \int\int d\vec{r}_1 d\vec{r}_2 a_c^*(\vec{r}_1-\vec{R}) \times a_{v'}^*(\vec{r}_2) g(r_{12}) a_{c'}(\vec{r}_2-\vec{R}) a_v(\vec{r}_1) \quad . \tag{7}$$

We further introduce the Fourier transform of $A_{cv}(\vec{k})$ at the lattice point $\vec{R}$,

$$A_{cv}(\vec{R}) = \sum_{\vec{k}} A_{cv}(\vec{k}) e^{i\vec{k}\cdot\vec{R}} \tag{8}$$

and we easily transform (2a) into

$$A_{cv}(\vec{R}_0) + \sum_{c'v'} \sum_{\vec{R}} A_{c'v'}(\vec{R}) \left[-\delta_{\sigma_c\sigma_{c'}} \delta_{\sigma_v\sigma_{v'}} Q(\vec{R}) \right.$$
$$+ \delta_{\sigma_c\sigma_v} \delta_{\sigma_{c'}\sigma_{v'}} \left(\sum_{\vec{R}'\neq 0} J_1(\vec{R}') e^{i\vec{q}\cdot\vec{R}'} \delta_{\vec{R},\vec{0}} \right.$$
$$\left. \left. + J_2(\vec{R}) \right) \right]_{cv,c'v'} G_{cv}(E, \vec{R}_0 - \vec{R}) = 0 \quad , \tag{9}$$

where

$$G_{cv}(E, \vec{R}_0 - \vec{R}) = N^{-1} \sum_{\vec{k}} \frac{e^{i\vec{k}\cdot(\vec{R}_0-\vec{R})}}{E_c(\vec{k}) - E_v(\vec{k}) - E} \tag{10}$$

is the Green's function for the c-v band pair, and we consider only the bound states for which $E \neq E_c(\vec{k}) - E_v(\vec{k})$.

The system of linear homogeneous equations (9) admits nonvanishing solutions in correspondence to the zeros of the determinant formed with the coefficients of the $A_{cv}(\vec{R})$. This is the Fredholm determinant of integral equation (2) and its order is equal to the number of $A_{cv}(\vec{R})$ different from zero which have to be considered. It is clear that this method is suitable when this number is small, i.e., when the number of interacting bands is small and the function $A_{cv}(\vec{R})$ is localized in space.

The one-site approximation is introduced by assuming $A_{cv}(\vec{R}) = 0$ if $R \neq 0$, i.e., by assuming that the electron and the hole are in the same unit cell. This approximation does not reduce the problem to a calculation of atomic excited states, because very important solid-state effects are present in Eq. (9) through the Wannier functions and the Green's functions, which contain the full band structure of the crystal. The one-site approximation in solid argon is justified by the very localized nature of the lowest exciton doublet. A reasonable estimate of the exciton size is provided by the pseudopotential calculation of Ref. 12, where the 1s-like wave function is characterized by a Bohr radius smaller than the nearest-neighbor distance. It should be noticed, furthermore, that this calculation probably overestimates the matrix elements of the Coulomb interaction between different centers, and therefore the size of the exciton, because of the long tail and great overlap of the approximate form chosen for the Wannier functions. This effect may also reduce the computed size of exciton states in krypton and xenon, and therefore justify the one-site approximation also in these cases, although the pseudopotential calculations[5,12] indicate convergence of the lowest eigenvalue only when the wave function extends over a few cells. A verification of the validity of the approximation in these latter cases, however, would be achieved by actually including the nearest-neighbor shell in Eq. (9) and thus explicitly checking the convergence of the eigenvalues. In the present paper we shall confine our quantitative analysis to argon, where a further confirmation of the validity of the one-site approximation will be found in the excellent agreement of the computed longitudinal and transverse exciton eigenvalues with experiment.

Once the one-site approximation is introduced in Eq. (9), the summation over $\vec{R}$ is dropped, and the

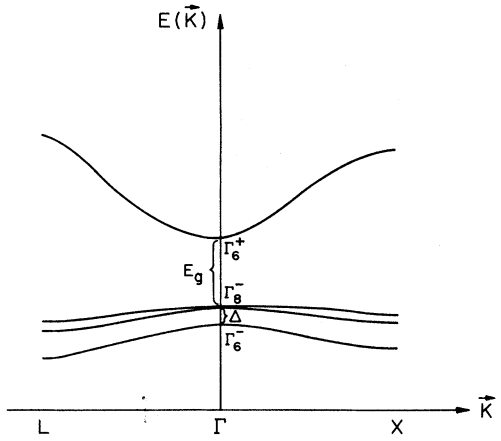

FIG. 1. Schematic band structure typical of solid rare gases and alkali halides. The states are classified in the notation of the double group and the spin-orbit splitting Δ at the top of the valence band is explicitly indicated (not to scale).

structure of the system of integral equations is determined by the number of valence and conduction bands considered and by their symmetry properties. To obtain explicit expressions, which can be actually computed in cases of interest, we must specify the band structure and take full advantage of symmetry.

III. BASIC EQUATIONS FOR SOLID RARE GASES AND ALKALI HALIDES

Let us consider the cases of solid rare gases and alkali halides, for which the structure of the lowest conduction band and of the highest valence bands is shown in Fig. 1. To proceed in the solution of our problem, we have to determine the properly symmetrized basis states for the expansion of the exciton functions. The exciton states result from the coupling between the twofold degenerate Γ_6^+ electron states and the spin-orbit split Γ_8^- and Γ_6^- hole states, fourfold and twofold degenerate, respectively, and therefore they belong to the irreducible representations contained in the direct products:

$$\Gamma_6^+ \otimes \Gamma_8^- = \Gamma_{12}' + \Gamma_{25} + \Gamma_{15} \,, \tag{11a}$$

$$\Gamma_6^+ \otimes \Gamma_6^- = \Gamma_1' + \Gamma_{15} \,. \tag{11b}$$

In Appendix A all the resulting exciton wave functions are written explicitly. However, we will consider here the eigenvalue problem for the Γ_{15} states only, because they are dipole allowed and therefore are the only states which can be excited in optical experiments.

For any row of the Γ_{15} irreducible representation, Eq. (9) becomes a 2×2 system which couples the two Γ_{15} states originating from Γ_8^- and Γ_6^- as indicated in Eq. (11). In this system, $Q(\vec{R})$ and $J_2(\vec{R})$ appear only for $\vec{R}=0$. For this value of $\vec{R}$, the overwhelming contribution to the integrals, as discussed in Sec. IV, comes from the regions of large overlap between the atomiclike valence Wannier function and the very localized spherically symmetric component of the conduction-band function. An estimate of $\epsilon(r_{12})$ based on the random-phase-approximation (RPA) calculation of Fry[14] shows that $\epsilon(r_{12})$ approaches exponentially its value for large r_{12}, 1.66, with a characteristic length of about 2 a.u. Considering that, owing to the large overlap of the Wannier functions mentioned above, screening effects are expected to be small, we assume $\epsilon(r_{12}) \simeq 1$. It should also be noticed that RPA breaks down for distances of the order of 1 a.u., and that any reliable calculation of $\epsilon(r_{12})$ in this range would make the numerical evaluation of Eqs. (5) and (7) unmanageable.

On the other hand, the integrals $J_1(\vec{R}')$ appear only for $\vec{R}' \neq 0$, and, in agreement with the preceding discussion, we can replace $\epsilon(r_{12})$ by $\epsilon_0 = 1.66$ in their evaluation. In the $\vec{q} \to 0$ limit, the summation over $\vec{R}'$ can be performed exactly if one considers only the dipole-dipole term[16] in the multipole expansion of J_1, as defined in Eq. (6). This polarization term, first introduced by Heller and Marcus,[16] is different for longitudinal and transverse excitons, and we denote it D_l and D_t, respectively.

With the basis functions of Appendix A we can finally evaluate the spin summations in Eq. (9) for the Γ_{15} states. As a result we obtain that, in the one-site approximation, the solutions are given by the equation

$$\begin{bmatrix} 1+[\frac{4}{3}(J+D_i)-Q]\,G_{8^-}(E) & -\frac{2}{3}\sqrt{2}\,(J+D_i)G_{8^-}(E) \\ -\frac{2}{3}\sqrt{2}\,(J+D_i)G_{6^-}(E) & 1+[\frac{2}{3}(J+D_i)-Q]\,G_{6^-}(E) \end{bmatrix} = 0 \tag{12}$$

where

$$Q = \int d\vec{r}_1\, d\vec{r}_2\, a_{\Gamma_1}^*(\vec{r}_1) p_X^*(\vec{r}_2) \frac{e^2}{r_{12}} a_{\Gamma_1}(\vec{r}_1) p_X(\vec{r}_2) \,, \tag{13}$$

$$J = \int d\vec{r}_1\, d\vec{r}_2\, a_{\Gamma_1}^*(\vec{r}_1) p_X^*(\vec{r}_2) \frac{e^2}{r_{12}} a_{\Gamma_1}(\vec{r}_2) p_X(\vec{r}_1) \,, \tag{14}$$

and the polarization term is given by[16]

$$D_i = \begin{cases} D_t = -(4\pi/3\epsilon_0)\, n_0 \mu_X^2 & \text{for transverse excitons } q \perp \mu, \\ D_l = (8\pi/3\epsilon_0)\, n_0 \mu_X^2 & \text{for longitudinal excitons } q \parallel \mu, \end{cases}$$

with

$$\mu_X = e \int d\vec{r}\, a^*_{\Gamma_1}(\vec{r})\, x\, p_X(\vec{r}) , \tag{16}$$

n_0 being the number of atoms in the unit volume. Furthermore,

$$G_{8^-}(E) = N^{-1} \sum_{\vec{k}} [E_{6^+}(\vec{k}) - E_{8^-}(\vec{k}) - E]^{-1} , \tag{17}$$

an analogous definition holding for G_{6^-}. We have labeled the energy bands with their symmetry at $\vec{k} = 0$, and the Wannier functions according to Appendix A.

We can gain some physical insight by looking at the structure of Eq. (12). If one ignores the off-diagonal elements for a moment, the energy separation of the two eigenstates is mostly contributed by the spin-orbit splitting Δ of the hole states, which enters Eq. (12) through the Green's functions. A small correction is introduced by the exchange terms. The correspondence between excitons and hole states is altered by the off-diagonal terms, which mix the two hole channels. It is worthwhile to point out that in the one-site approximation the Coulomb interaction between the electron and the hole does not mix the two excitation channels. Therefore the exchange term alone is responsible for the anomalies in the splitting and the intensity ratio of the two peaks, and such anomalies are more important as the ratio of $(J + D_i)$ to Δ increases.

IV. CALCULATION OF GREEN'S FUNCTIONS, WANNIER FUNCTIONS, AND COULOMB AND EXCHANGE INTEGRALS FOR SOLID ARGON

At this point, we undertake the task of evaluating the quantities entering Eq. (12) for the specific case of solid argon, in order to be able to compute the energy of the exciton states. Our aim is not so much a calculation which includes the fine details of the band structure, but a calculation which takes into account the basic features of the band structure and of the Bloch functions throughout the Brillouin zone. The eigenvalues of Eq. (12), in fact, depend on $E(\vec{k})$ and on the Bloch functions through integrated quantities only, as already pointed out.

Let us now consider the Green's function $G(E)$. It is convenient to rewrite $G(E)$ as a function of the binding energy $E_b = E_g - E$, E_g being the energy gap:

$$G(E_b) = N^{-1} \sum_{\vec{k}} \frac{1}{E_{cv}(\vec{k}) + E_b} , \tag{18}$$

with

$$E_{cv}(\vec{k}) = E_c(\vec{k}) - E_v(\vec{k}) - E_g . \tag{19}$$

In order to reproduce the salient features of $E_{cv}(\vec{k})$ in a simple analytical form, suitable for a fast computation of Eq. (18), we use a three-term tight-binding interpolation formula:

$$\begin{aligned} E_{cv}(\vec{k}) = {} & 3(E_0 + E_1 + E_2) \\ & - E_0(\cos x \cos y + \cos y \cos z + \cos z \cos x) \\ & - E_1(\cos 2x + \cos 2y + \cos 2z) \\ & - E_2(\cos 2x \cos y \cos z + \cos 2y \cos x \cos z \\ & + \cos 2z \cos x \cos y) , \end{aligned} \tag{20}$$

with $x = k_x a/2$, $y = k_y a/2$, $z = k_z a/2$, a being the lattice parameter. The three parameters E_0, E_1, E_2 are determined by the conduction-band effective mass[17,18] at $\vec{k} = 0$, and the calculated values[19] of $E_{cv}(\vec{k})$ at the X and L points, namely,[17,18]

$$m^*(\Gamma) = 0.48 m_0$$

and[19]

$$E_c(X) = 2.89 \text{ eV} , \quad E_c(L) = 3.29 \text{ eV} ,$$

to which an average valence bandwidth (0.8 eV) is added to obtain $E_{cv}(\vec{k})$. The value of the spin-orbit splitting of the valence band at Γ, $\Delta = 0.18$ eV, is taken from the band-structure calculation of Rössler,[17] and is close to the corresponding atomic value.[11,20]

The Green's function $G_{8^-}(E)$ is plotted in Fig. 2, together with two more crude approximations, in which the bands are approximated by a free-electron-like formula, the effective mass being taken as the computed value at Γ or so to give the correct value of $E_{cv}(\vec{k})$ at L. As one can expect, the function corresponding to Eq. (20), which fits both the correct mass and the bandwidth, lies in between the two spherical approximations. The importance of fitting both effective mass and bandwidth is self-evident from Fig. 2.

Let us now turn our attention to the Wannier functions and their matrix elements Q, J, and μ_X. The Wannier functions of the valence bands for solid argon can be replaced by the $3p$ atomic functions, as obtained, e.g., in analytical form by Watson and Freeman,[21] because they are very localized and the overlap between neighboring sites is negligible.[22] On the other hand, this is not the case for the $4s$ atomic functions, and we must resort to another technique to obtain the Wannier function for the conduction band, $a_{\Gamma_1}(\vec{r})$.

Following the method suggested by Miasek,[23] we start from the transform of a set of plane waves

$$\chi(\vec{r}) = \frac{1}{N\sqrt{\Omega_0}} \sum_{\vec{k} \in \text{B Z}} e^{i\vec{k}\cdot\vec{r}} , \tag{21}$$

which can be computed exactly for the fcc lattice.[23] This function is then orthogonalized to the core and

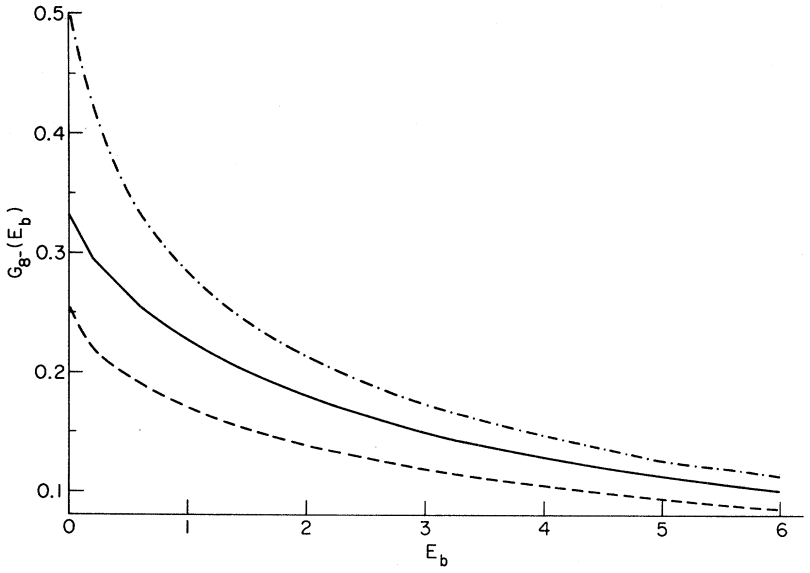

FIG. 2. Green's function $G_{8^-}(E_b)$ as computed by fitting band-structure calculations (solid line) and from a free-electron-like approximation, with an effective mass determined by the bandwidth (dash-dotted line) or by the effective mass at the edge (dashed line). (E_b in eV).

valence atomic functions on the origin site as well as on the nearest-neighbor sites. The overlap integrals are computed by expanding $\chi(\vec{r})$ and the appropriate combinations of atomic functions in cubic harmonics of Γ_1 symmetry[24] (see Appendix B). The expansion coefficients are obtained by Houston's method[23] and the integration is performed, for near neighbors, with the help of Löwdin's α-function expansion.[25] More distant neighbors need not be included, the overlap with second neighbors already being negligible, as discussed in Appendix B, where all the details of the calculation are given. The function thus obtained has therefore all the orthogonality properties of Wannier functions, together with the nodal structure of the atomic 4s function, resulting from the orthogonalization to the lower atomic orbitals of the same site.

In order to compute the Coulomb and exchange integrals as defined in Eqs. (13) and (14) in a straightforward way, the conduction-band Wannier function is approximated by an expansion in cubic harmonics, with the procedure outlined in Appendix B for overlap integrals between functions of Γ_1 symmetry. In Figs. 3 and 4 the function $ra_{\Gamma_1}(\vec{r})$ is shown along the [100] and [110] directions, together with the cubic harmonic expansion, and with the spherically symmetric contribution $ra_0(r)$. The expansion converges fairly well, except in the neighborhood of the nearest atomic site ($r = 7.10$ a.u.). As it is to be expected, the contribution of neighboring sites destroys the spherical symmetry of the function which dominates until $r \cong 4$ a.u. Figure 5 shows a comparison of the spherical term with the 4s atomic function computed by Knox.[26] Notice the coincidence of the nodes[27] near the origin and the stronger localization[28] of the Wannier function.

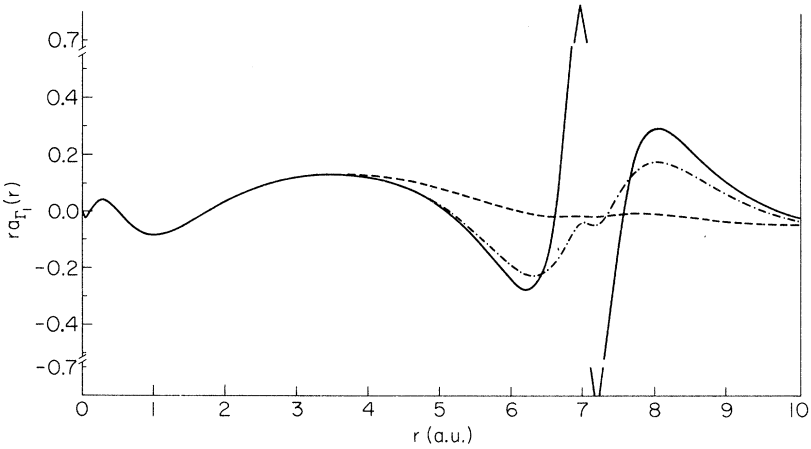

FIG. 3. Wannier function of the Ar conduction band, $ra_{\Gamma_1}(r)$ along the [110] direction (solid line), compared with an expansion in spherical harmonics up to $l = 12$ (dash-dotted line) and with its spherically symmetric component (dashed line).

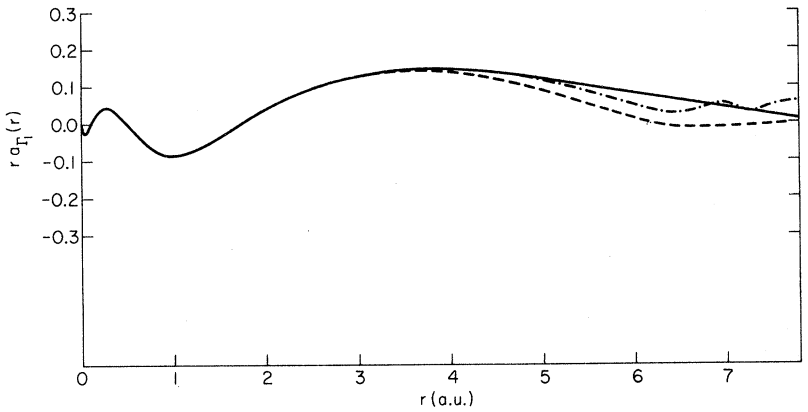

FIG. 4. Same as Fig. 3, but along the [100] direction.

The expansion of a_{Γ_1} in cubic and therefore spherical harmonics[24] allows us to decompose Q and J in separate contributions from each angular momentum component of the conduction-band function. They are listed separately in Table I, to show the convergence of the integrals with increasing l quantitatively. More than 91 and 99% of the values of Q and J, respectively, as associated with the s component alone, which, owing to its strong localization (see Fig. 5), overlaps greatly with the $3p$ function. The integrals are therefore dominated by the small-r_{12} region, thus justifying our neglect of screening effects for $\vec{R}=0$. In Table I the value of the parameter $n_0\mu_X^2$, occurring in the dipolar term D_i, is also given.

V. EXCITON SPECTRUM OF SOLID ARGON

We can now use the parameters computed in Sec. IV and the Green's function of Fig. 2 to solve Eq. (12) for solid argon. The values of all the quantities of interest are listed together in Table II for convenience. In Table III the energies of the lowest Γ_{15} excitons ($n=1$ in the conventional effective-mass notation) are given. The longitudinal and transverse modes are obtained inserting D_l or D_t in Eq. (12). We defer the comparison of these theoretical results with experiment until Sec. VI. In Table III the relative contributions of the $\Gamma_{8-}-\Gamma_{6+}$ and $\Gamma_{6-}-\Gamma_{6+}$ band edges to the two transverse exciton eigenfunctions $|A_i^{(8-)}|^2$ and $|A_i^{(6-)}|^2$ are also given.

The results of Table III indicate a considerable admixture of the two hole states induced by the exchange interaction. As a consequence, the splitting of the two states differs from the spin-orbit splitting of the valence band and the intensity ratio is different from 2:1. It is easy to obtain for the intensity ratio the expression

$$\frac{I_1}{I_2}=\frac{1+|A_1^{(8-)}|^2-2\sqrt{2}\,A_1^{(8-)}A_1^{(6-)}}{2-|A_1^{(8-)}|^2+2\sqrt{2}\,A_1^{(8-)}A_1^{(6-)}}\,. \tag{22}$$

[Notice that $A^{(8-)}A^{(6-)}>0$ with our choice of the basis functions, Eqs. (A7) and (A8).] Equation (22) shows how strongly the intensity ratio can be modified by the admixture of the two excitation channels. This effect has been discussed by Onodera and Toyozawa[4] within the framework of the effective-mass approximation.

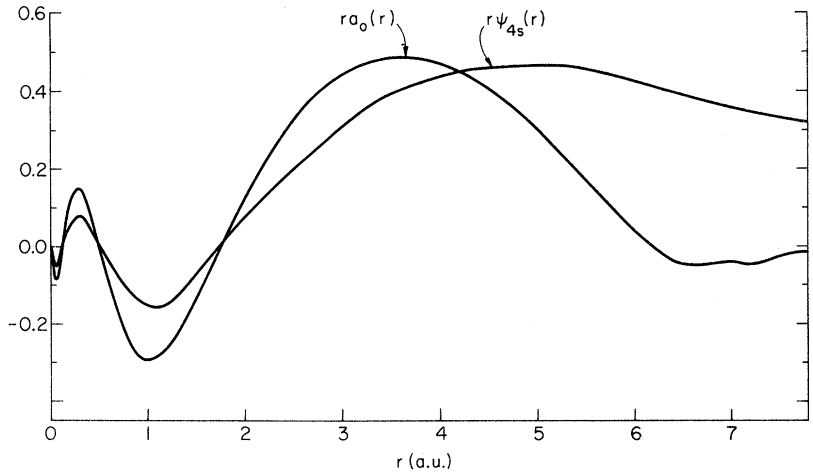

FIG. 5. Spherical contribution to the Wannier function compared with the 4s atomic Ar function ψ_{4s}, as computed by Knox in Ref. 26.

TABLE I. Values (in eV) of the Coulomb and exchange integrals Q and J for solid Ar, and contributions from the different angular momentum components. Also shown is the value of the quantity $n_0\mu_x^2$ (in eV), entering Heller and Marcus's expression (Ref. 16) of the dipolar sum.

l	0	4	6	8	10	Total
Q	5.312	0.117	0.286	0.082	0.005	5.802
J	0.204	4×10^{-4}	9×10^{-4}	2×10^{-4}	$\sim10^{-6}$	0.205
$n_0\mu_x^2$	0.016					0.016

In order to better understand the dependence of the doublet splitting on the relative magnitude of the exchange interaction and on the spin-orbit separation of the valence bands, we plot this quantity in Fig. 6 as a function of the ratio

$$\eta = 2(J + D_t)/\Delta \,, \tag{23}$$

the other parameters being those appropriate for solid argon and discussed above. It can be noticed from Fig. 6 that the splitting is practically unchanged as long as $\eta \lesssim 1$, but is rapidly increasing with η for $\eta > 1$.

In Fig. 7 the intensity ratio I_1/I_2 is also plotted as a function of η. It is interesting to notice that even in the small η region, where the doublet splitting is unchanged, the intensity ratio is strongly dependent on η. For $\eta \cong 0.3$ the two peaks have the same intensity. For $\eta > 2$, only the second peak is observable, because the first is essentially a triplet state. This explains the lack of doublet structure in the spectrum of Ne,[9] where the spin-orbit splitting is much smaller than the exchange integral.

The general behavior shown in Figs. 6 and 7 does not depend greatly on the other parameters of the band structure. Quite similar curves can be obtained by varying Q and the width of the valence and conduction bands. Therefore, the qualitative conclusions obtained here can be extended to the other rare gases. It is then easy to understand why, going from argon to krypton and to xenon, the relative intensity of the second peak decreases and approaches the ratio 1 : 2 as the spin-orbit splitting increases with atomic number.

VI. CONCLUSIONS

We briefly summarize the results obtained in the previous sections in order to draw some general conclusions.

TABLE II. Values (in eV) of the energy parameters entering Eq. (12) and of the spin-orbit splitting Δ. The latter is taken from the band-structure calculation of Ref. 17.

Q	J	D_t	D_l	Δ
5.802	0.205	−0.040	0.081	0.18

TABLE III. Theoretical and experimental values of the exciton binding energies $E_b = E_g - E$ in solid argon (in eV), and wave-function admixture coefficients. The binding energies are obtained assuming a band gap of 14.16 eV (Haensel *et al.*, Ref. 9). The theoretical relative intensities of the two transverse excitons are also given in the bottom row.

	$\Gamma_{15}(1)t$	$\Gamma_{15}(2)t$	$\Gamma_{15}(1)l$	$\Gamma_{15}(2)l$
E_b(theory)	2.12	1.84	2.10	1.65
E_b(expt.)	2.16[a]	1.86[a]	2.11[c]	1.70[c]
	2.06[b]	1.81[b]		
$\lvert A_8\rangle\rvert^2$	0.696	0.304		
$\lvert A_6\rangle\rvert^2$	0.304	0.696		
Relative intensity	1	6.5		

[a] G. Baldini, Ref. 9.
[b] R. Haensel, G. Keitel, E. E. Koch, M. Skibowsky, and P. Schreiber, Ref. 9.
[c] O. Bostanjoglo and L. Schmidt, Ref. 10.

(a) A formulation of the exciton problem suitable to deal with intermediate binding is derived, in which the energy bands $E_n(\vec{k})$ enter explicitly, and the full electron-hole interaction is computed from Wannier functions. Longitudinal and transverse excitons of given symmetry can be obtained as solutions of simple Fredholm equations which depend on easily computable integrals. The problem is greatly simplified if the electron and the hole can be assumed to be confined to the same cell. The exciton energies can then be obtained in terms of a few parameters which can be computed from first

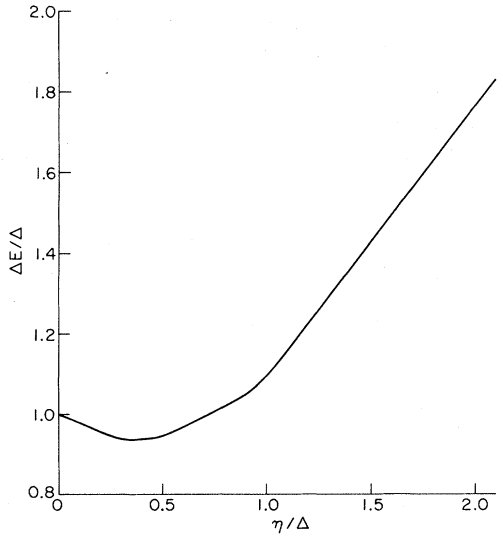

FIG. 6. Separation of the exciton doublet ΔE as a function of $\eta = 2(J+D)/\Delta$. Energies are in units of the valence-band spin-orbit splitting.

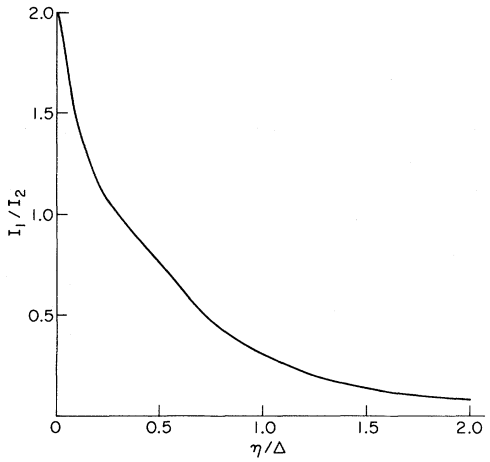

FIG. 7. Intensity ratio I_1/I_2 (see text) of the exciton doublet as a function of $\eta = 2(J+D)/\Delta$. The quantities Q and $G(E_b)$ are those appropriate to solid Ar and discussed in the text.

principles.

(b) The calculations performed for solid argon show that the one-site approximation is fully justified in this case. This is because the Wannier function of the conduction band is much more localized than the corresponding 4*s* atomic function. The agreement between theory and experiment (Table III) which was obtained in this case is remarkably good, particularly when one considers that this is a completely *ab initio* calculation with no adjustable parameters.

(c) The separation and the relative intensities of the lowest longitudinal and transverse exciton doublet (the two $n=1$ excitons, in the Wannier-Mott picture) are completely understood in terms of the ratio of the exchange interaction to the spin-orbit splitting of the valence band.

The higher exciton states could also be computed by the present method, but an extension to a few neighboring cells would be required. The approach would converge, for higher and higher excitons, to the effective-mass approximation. Probably, the latter method would give satisfactory results for $n=2$ already, at least as far as the energy eigenvalue is concerned. However, whatever agreement can be found between the $n=1$ effective-mass eigenvalues and the lowest exciton states is completely fortuitous, because the present calculation shows that the exciton radius is of the order of the unit-cell dimensions. There is therefore a strong correlation with the lowest atomic doublet, but with very important solid-state effects, which are explicitly taken into account in our calculation.

We believe that the results obtained indicate that a full understanding of the excitonic structure of the whole family of solid rare gases is at hand. A calculation of the Wannier functions has to be performed for Ne, Kr, and Xe, but it is already possible on the basis of Figs. 6 and 7 to correlate qualitatively some properties of the lowest doublet to the spin-orbit splitting and therefore to atomic number. As the overlap between atomic functions becomes larger, it may be necessary to use different methods of calculation of the Wannier function of the valence bands, such as the one advocated by Kohn,[29] and to go beyond the one-site approximation.

A further problem to which the present approach is applicable is that of core excitons which are produced by synchrotron radiation; this will be discussed in a separate paper.[30] In this case the core wave functions are more localized and the one-site approximation is even better justified.

Extensions to other materials, such as the alkali halides, are also possible. It is worthwhile to notice that the "transfer model"[31] would be included in the one-site approximation, as the anion and the cation are in the same unit cell. In these materials, however, more attention should be paid to screening effects, which are more complicated than in rare-gas solids.

ACKNOWLEDGMENTS

The authors are grateful to Professor R. S. Knox for providing them with unpublished results of R. S. Knox and M. Miasek on the Wannier function of Ar, and for several discussions.

APPENDIX A: EXCITON BASIS STATES

In the Wannier representation, any direct exciton wave function in the one-site approximation can be written as

$$|\Psi_{\vec{q}=0}\rangle = \sum_{c=1}^{N_c}\sum_{v=1}^{N_v} A_{c,v}(\vec{0})\,|\,c,\,v,\,\vec{0}\rangle_{\vec{q}=0}\ , \tag{A1}$$

where the ket represents the Slater determinant corresponding to the excited state of the N-particle system, where an electron in the Wannier state $a_v(\vec{r})$ has been excited to the Wannier state $a_c(\vec{r})$ localized in the same unit cell. In the particular case where the band structure is that given in Fig. 1, the sums in (A1) run over the degenerate conduction states belonging to the Γ_6^+ representation of the double cubic group ($N_c=2$) and the degenerate valence states belonging to the Γ_8^- representation or the Γ_6^- representation ($N_v=6$).

It is clear that an individual exciton wave function referring to a specific band-edge electron-hole pair belongs to a reducible representation given by the direct product of the irreducible representation of its component, namely,

$$\Gamma_{\text{exc}} = \Gamma_e \times \Gamma_h\ . \tag{A2}$$

Then, we have to determine the irreducible repre-

sentations contained in the product (A2), and then the symmetrized exciton basis states transforming as the rows of such representations. The electron-hole couplings decompose in the following way:

$$\Gamma_8^- \times \Gamma_6^+ = \Gamma_{25} + \Gamma_{12}' + \Gamma_{15} ,$$
$$\Gamma_6^- \times \Gamma_6^+ = \Gamma_1' + \Gamma_{15} . \tag{A3}$$

In order to obtain the corresponding wave functions, we have simply to know the generalized Clebsch-Gordan coefficients[32] $\alpha_{c,v}^{\lambda,l}$ in the general expansion

$$|\lambda l\rangle = \sum_{c=1}^{2} \sum_{v=1}^{6} \alpha_{c,v}^{\lambda,l} |c, v, \vec{0}\rangle , \tag{A4}$$

where λ and l label the irreducible representation and its lth row, respectively.

In the following we substitute the Slater ket in (A4) with the product of the excited electron state and of the hole state, since the two-particle representation is completely equivalent to the many-body representation, as one can see in detail in Ref. 33. We obtain the following exciton basis states: From the coupling $\Gamma_8^- - \Gamma_6^+$

$$|d_1\rangle = \frac{1}{\sqrt{2}}\left[\frac{1}{2}\left(\frac{1}{\sqrt{2}}(p_x - ip_y)\beta\right) a_{\Gamma_1}\beta + \frac{\sqrt{3}}{2}\left(-\frac{1}{\sqrt{6}}(p_x - ip_y)\alpha - \sqrt{\frac{2}{3}}p_z\beta\right)a_{\Gamma_1}\alpha \right.$$
$$\left. + \frac{\sqrt{3}}{2}\left(-\frac{1}{\sqrt{6}}(p_x + ip_y)\beta + \sqrt{\frac{2}{3}}p_z\alpha\right)a_{\Gamma_1}\beta + \frac{1}{2}\left(\frac{1}{\sqrt{2}}(p_x + ip_y)\alpha\right)a_{\Gamma_1}\alpha\right] ,$$
$$|d_2\rangle = \frac{i}{\sqrt{2}}\left[\frac{1}{2}\left(\frac{1}{\sqrt{2}}(p_x - ip_y)\beta\right)a_{\Gamma_1}\beta + \frac{\sqrt{3}}{2}\left(-\frac{1}{\sqrt{6}}(p_x - ip_y)\alpha - \sqrt{\frac{2}{3}}p_z\beta\right)a_{\Gamma_1}\alpha \right.$$
$$\left. - \frac{\sqrt{3}}{2}\left(-\frac{1}{\sqrt{6}}(p_x + ip_y)\beta + \sqrt{\frac{2}{3}}p_z\alpha\right)a_{\Gamma_1}\beta - \frac{1}{2}\left(\frac{1}{\sqrt{2}}(p_x + ip_y)\alpha\right)a_{\Gamma_1}\alpha\right] ,$$
$$|d_3\rangle = -\frac{1}{\sqrt{2}}\left[\frac{1}{\sqrt{2}}\left((p_x - ip_y)\beta\, a_{\Gamma_1}\alpha\right) - \frac{1}{\sqrt{2}}\left((p_x + ip_y)\alpha\, a_{\Gamma_1}\beta\right)\right] \tag{A5}$$

for Γ_{25};

$$|\delta_1\rangle = \frac{i}{\sqrt{2}}\left[\left(-\frac{1}{\sqrt{6}}(p_x - ip_y)\alpha - \sqrt{\frac{2}{3}}p_z\beta\right)a_{\Gamma_1}\beta + \left(-\frac{1}{\sqrt{6}}(p_x + ip_y)\beta + \sqrt{\frac{2}{3}}p_z\alpha\right)a_{\Gamma_1}\alpha\right] , \tag{A6}$$

$$|\delta_2\rangle = \frac{i}{\sqrt{2}}\left(\frac{1}{\sqrt{2}}(p_x - ip_y)\beta\, a_{\Gamma_1}\alpha + \frac{1}{\sqrt{2}}(p_x + ip_y)\alpha\, a_{\Gamma_1}\beta\right)$$

for Γ_{12}';

$$|X\rangle = \frac{1}{\sqrt{2}}\left[-\frac{\sqrt{3}}{2}\left(\frac{1}{\sqrt{2}}(p_x - ip_y)\beta\right)a_{\Gamma_1}\beta + \frac{1}{2}\left(-\frac{1}{\sqrt{6}}(p_x - ip_y)\alpha - \sqrt{\frac{2}{3}}p_z\beta\right)a_{\Gamma_1}\alpha \right.$$
$$\left. + \frac{1}{2}\left(-\frac{1}{\sqrt{6}}(p_x + ip_y)\beta + \sqrt{\frac{2}{3}}p_z\alpha\right)a_{\Gamma_1}\beta - \frac{\sqrt{3}}{2}\left(\frac{1}{\sqrt{2}}(p_x + ip_y)\alpha\right)a_{\Gamma_1}\alpha\right] ,$$
$$|Y\rangle = \frac{i}{\sqrt{2}}\left[-\frac{\sqrt{3}}{2}\left(\frac{1}{\sqrt{2}}(p_x - ip_y)\beta\right)a_{\Gamma_1}\beta + \frac{1}{2}\left(-\frac{1}{\sqrt{2}}(p_x - ip_y)\alpha - \sqrt{\frac{2}{3}}p_z\beta\right)a_{\Gamma_1}\alpha \right.$$
$$\left. - \frac{1}{2}\left(-\frac{1}{\sqrt{6}}(p_x + ip_y)\beta + \sqrt{\frac{2}{3}}p_z\alpha\right)a_{\Gamma_1}\beta + \frac{\sqrt{3}}{2}\left(\frac{1}{\sqrt{2}}(p_x + ip_y)\alpha\right)a_{\Gamma_1}\alpha\right] , \tag{A7}$$
$$|Z\rangle = \frac{\sqrt{2}}{2}\left(-\frac{1}{\sqrt{6}}(p_x - ip_y)\alpha - \sqrt{\frac{2}{3}}p_z\beta\right)a_{\Gamma_1}\beta - \frac{\sqrt{2}}{2}\left(-\frac{1}{\sqrt{6}}(p_x + ip_y)\beta + \sqrt{\frac{2}{3}}p_z\alpha\right)a_{\Gamma_1}\alpha$$

for Γ_{15}. From the coupling $\Gamma_6^- - \Gamma_6^+$

$$|\xi\rangle = \frac{1}{\sqrt{2}}\left[\left(-\frac{1}{\sqrt{3}}p_z\beta + \frac{1}{\sqrt{3}}(p_x - ip_y)\alpha\right)a_{\Gamma_1}\alpha + \left(\frac{1}{\sqrt{3}}p_z\alpha + \frac{1}{\sqrt{3}}(p_x + ip_y)\beta\right)a_{\Gamma_1}\beta\right] ,$$
$$|\eta\rangle = -\frac{i}{\sqrt{2}}\left[\left(-\frac{1}{\sqrt{3}}p_z\beta + \frac{1}{\sqrt{3}}(p_x - ip_y)\alpha\right)a_{\Gamma_1}\alpha - \left(\frac{1}{\sqrt{3}}p_z\alpha + \frac{1}{\sqrt{3}}(p_x + ip_y)\beta\right)a_{\Gamma_1}\beta\right] , \tag{A8}$$
$$|\zeta\rangle = -\frac{1}{\sqrt{2}}\left(-\frac{1}{\sqrt{3}}p_z\beta + \frac{1}{\sqrt{3}}(p_x - ip_y)\alpha\right)a_{\Gamma_1}\beta + \frac{1}{\sqrt{2}}\left(\frac{1}{\sqrt{3}}p_z\alpha + \frac{1}{\sqrt{3}}(p_x + ip_y)\beta\right)a_{\Gamma_1}\alpha$$

for Γ_{15}';

$$|\epsilon\rangle = \frac{i}{\sqrt{2}}\left[\left(\frac{1}{\sqrt{3}}(p_x - ip_y)\alpha - \frac{1}{\sqrt{3}}p_z\beta\right)a_{\Gamma_1}\beta + \left(\frac{1}{\sqrt{3}}(p_x + ip_y)\beta + \frac{1}{\sqrt{3}}p_z\alpha\right)a_{\Gamma_1}\alpha\right] \tag{A9}$$

for Γ_{15}^i

In all the above expressions, (A5)–(A9), the functions p_x, p_y, p_z are Wannier functions transforming as the rows of the Γ_{15} representation and a_{Γ_1} is the Wannier function transforming as the Γ_1 representation of the simple cubic group. The spin functions $\binom{1}{0}$ and $\binom{0}{1}$ are denoted by α and β, respectively.

APPENDIX B: CALCULATION OF THE WANNIER FUNCTION OF THE LOWEST CONDUCTION BAND IN Ar

We follow the method suggested by Miasek[23] to compute the Wannier function corresponding to the conduction band, from Bloch functions approximated by a single plane wave orthogonalized to all the core and valence states of argon. In the nearest-neighbor approximation, the Wannier function (of Γ_1 symmetry) assumes the following form:

$$a(\vec{r}) = \chi(\vec{r}) - \sum_{n=1}^{3} B_{ns}(0)\phi_{ns}(\vec{r}) - \sum_{n=1}^{3} C_{ns}(R)\Phi_{ns}(\vec{r}) - \sum_{m=2}^{3} C_{mp}(R)\Phi_{mp}(\vec{r}), \tag{B1}$$

where

$$\chi(\vec{r}) = (N\sqrt{\Omega_0})^{-1}\sum_{\vec{k}\in BZ} e^{i\vec{k}\cdot\vec{r}}, \tag{B2}$$

$$\Phi_{ns}(\vec{r}) = \frac{b_{ns}}{\sqrt{12}}\sum_{\vec{R}=1}^{12}\phi_{ns}(\vec{r} - \vec{R}), \tag{B3}$$

and

$$\begin{aligned}\Phi_{mp}(\vec{r}) = \frac{b_{mp}}{\sqrt{24}}\{&[\phi_{mx}(\vec{r} - \vec{R}_1) + \phi_{mx}(\vec{r} - \vec{R}_4) + \phi_{mx}(\vec{r} - \vec{R}_2) + \phi_{mx}(\vec{r} - \vec{R}_5) - \phi_{mx}(\vec{r} - \vec{R}_{10}) - \phi_{mx}(\vec{r} - \vec{R}_7) - \phi_{mx}(\vec{r} - \vec{R}_8)\\ &- \phi_{mx}(\vec{r} - \vec{R}_{11})] + [\phi_{my}(\vec{r} - \vec{R}_1) + \phi_{my}(\vec{r} - \vec{R}_{10}) + \phi_{my}(\vec{r} - \vec{R}_3) + \phi_{my}(\vec{r} - \vec{R}_6) - \phi_{my}(\vec{r} - \vec{R}_4) - \phi_{my}(\vec{r} - \vec{R}_7)\\ &- \phi_{my}(\vec{r} - \vec{R}_{12}) - \phi_{my}(\vec{r} - \vec{R}_9)] + [\phi_{mz}(\vec{r} - \vec{R}_2) + \phi_{mz}(\vec{r} - \vec{R}_{11}) + \phi_{mz}(\vec{r} - \vec{R}_3) + \phi_{mz}(\vec{r} - \vec{R}_{12}) - \phi_{mz}(\vec{r} - \vec{R}_5)\\ &- \phi_{mz}(\vec{r} - \vec{R}_8) - \phi_{mz}(\vec{r} - \vec{R}_6) - \phi_{mz}(\vec{r} - \vec{R}_9)]\},\end{aligned} \tag{B4}$$

with

$$\vec{R}_1 = \tfrac{1}{2}a(1, 1, 0), \quad \vec{R}_4 = \tfrac{1}{2}a(1, \bar{1}, 0),$$

$$\vec{R}_2 = \tfrac{1}{2}a(1, 0, 1), \quad \vec{R}_5 = \tfrac{1}{2}a(1, 0, \bar{1}),$$

$$\vec{R}_3 = \tfrac{1}{2}a(0, 1, 1), \quad \vec{R}_6 = \tfrac{1}{2}a(0, 1, \bar{1}),$$

and

$$\vec{R}_{n+6} = -\vec{R}_n. \tag{B5}$$

In Eq. (B1) $B_{ns}(0)$, $C_{ns}(R)$, and $C_{mp}(R)$ are the overlap integrals between the $\chi(\vec{r})$ function and the s-core atomic functions $\phi_{ns}(\vec{r})$ and the symmetrized combinations (B3) and (B4) of s- and p-core wave functions, respectively. In our case $R = |\vec{R}| = 7.10$ a.u. In Eq. (B2) Ω_0 is the volume of the unit cell in the fcc lattice, and, finally, in Eqs. (B3) and (B4) b_{ns} and b_{mp} are normalization constants.

In computing the orthogonalization coefficients $C_{ns}(R)$ and $C_{mp}(R)$ we expand the functions (B2), (B3), and (B4), all of Γ_1 symmetry, in cubic harmonics, namely,

$$\chi(\vec{r}) = \sum_i g_i(r)K_i(\theta, \phi), \tag{B6a}$$

$$\Phi_{ns\,(mp)}(\vec{r}) = \sum_i \Psi_i^{ns\,(mp)}(r)K_i(\theta, \phi). \tag{B6b}$$

The expansions were truncated at $i = 6$, after verifying that very good convergence was achieved. The coefficients $g_i(r)$ were computed following the six-terms Houston method, as applied by Miasek,[23] after inverting the cubic harmonics matrix by computer. The explicit computation of the integrals, which are linear combinations of two-center integrals, required general formulas allowing us to separate the dependence on the relative distance from that on the relative orientation of the two centers, for cubic harmonics of arbitrary order.[34] We also took advantage of Löwdin's α-function expansion.[25]

A similar computation of overlap integrals between $\chi(\vec{r})$ and the core wave functions centered on next nearest neighbors ($R = 10.05$ a.u.) gave results about two orders of magnitude smaller. Therefore, it is possible to retain only the nearest-neighbor contribution to the Wannier functions.

Based on work supported in part by the Italian National Research Council (CNR) through Gruppo Nazionale di Struttura della Materia and by the U. S. Army Research Office, Durham, N. C., under Contract No. DA-HC04-74-C-0005.

[1]See, for instance, R. S. Knox, *Theory of Excitons* (Academic, New York, 1963); F. Bassani and G. Pastori-Parravicini, *Electronic States and Optical Transitions in Solids* (Pergamon, New York, 1974), Chap. 6; J. J. Hopfield, in *Quantum Optics*, edited by R. J. Glauber (Academic, New York, 1969), p. 340.

[2]S. Nikitine, in *Optical Properties of Solids*, edited by S. Nudelman and S. S. Mitra (Plenum, New York, 1969), p. 197.

[3]S. Nikitine, C. R. Acad. Sci. (Paris) 240, 1415 (1955); J. A. Deverin, Nuovo Cimento B 63, 1 (1969); A. Baldereschi and M. G. Diaz, Nuovo Cimento B 68, 217 (1970).

[4]A. Baldereschi and N. O. Lipari, Phys. Rev. B 3, 439 (1971); 3, 2497 (1971); Y. Onodera and Y. Toyozawa, J. Phys. Soc. Jpn. 22, 833 (1967).

[5]J. Hermanson and J. C. Phillips, Phys. Rev. 150, 652 (1966); J. Hermanson, Phys. Rev. 150, 660 (1966).

[6]A. S. Davydov, *Theory of Molecular Excitons* (McGraw-Hill, New York, 1962).

[7]M. Altarelli and F. Bassani, J. Phys. C 4, L328 (1971).

[8]M. Altarelli and F. Bassani, in *Proceedings of the XI International Conference on the Physics of Semiconductors* (Polish Scientific Publishers, Warsaw, 1972), p. 196.

[9]G. Baldini, Phys. Rev. 128, 1562 (1962); J. F. O'Brien and K. J. Teegarden, Phys. Rev. Lett. 17, 919 (1966); I. T. Steinberger and O. Schnepp, Solid State Commun. 5, 417 (1967); R. Haensel, G. Keitel, E. E. Koch, M. Skibowsky, and P. Schreiber, Phys. Rev. Lett. 23, 1160 (1969); Opt. Commun. 2, 59 (1970); I. T. Steinberger, C. Atluri, and O. Schnepp, J. Chem. Phys. 52, 2723 (1970); R. Haensel, G. Keitel, E. E. Koch, N. Kosuch, and M. Skibowsky, Phys. Rev. Lett. 25, 1281 (1970).

[10]O. Bostanjoglo and L. Schmidt, Phys. Lett. 22, 123 (1966); P. Keil, Z. Naturforsch. A 21, 503 (1966); Z. Phys. 214, 251 (1968); L. Schmidt, Phys. Lett. A 36, 87 (1971).

[11]R. S. Knox, J. Phys. Chem. Solids 9, 265 (1959).

[12]U. Rössler and O. Schutz, Phys. Status Solidi 56, 483 (1973).

[13]Y. Takeuti, Prog. Theor. Phys. 18, 421 (1957).

[14]H. Haken, Nuovo Cimento 3, 1230 (1956); W. Kohn, Phys. Rev. 105, 509 (1957); J. Hubbard, Proc. R. Soc. A 244, 199 (1958); A. Morita, M. Azuma, and H. Nara, J. Phys. Soc. Jap. 17, 1570 (1962); Y. Abe, Y. Osaka, and A. Morita, J. Phys. Soc. Jpn. 17, 1576 (1962); J. L. Fry, Phys. Rev. 179, 892 (1969).

[15]C. Horie, Prog. Theor. Phys. 21, 113 (1959).

[16]W. R. Heller and A. Marcus, Phys. Rev. 84, 809 (1951).

[17]U. Rössler, Phys. Status Solidi 42, 345 (1970).

[18]A. B. Kunz and D. J. Mickish, Phys. Rev. B 8, 779 (1973).

[19]N. O. Lipari, Phys. Rev. B 6, 4071 (1972).

[20]F. Herman and S. Skillman, *Atomic Structure Calculations* (Prentice-Hall, Englewood Cliffs, N. J., 1963).

[21]R. E. Watson and A. J. Freeman, Phys. Rev. 123, 521 (1961).

[22]R. S. Knox and F. Bassani, Phys. Rev. 124, 652 (1961).

[23]M. Miasek, J. Math. Phys. 7, 139 (1966).

[24]C. J. Bradley and A. P. Cracknell, *The Mathematical Theory of Symmetry in Solids* (Oxford U. P., Oxford, England, 1972), Chap. 2; F. M. Mueller and M. G. Priestley, Phys. Rev. 148, 638 (1966).

[25]P. O. Löwdin, Adv. Phys. 5, 1 (1956).

[26]R. S. Knox, Phys. Rev. 110, 375 (1958).

[27]G. H. Wannier, Phys. Rev. 52, 191 (1937).

[28]E. I. Blount, in *Solid State Physics*, edited by F. Seitz, D. Turnbull, and H. Ehrenreich (Academic, New York, 1962), Vol. 13, p. 305.

[29]W. Kohn, Phys. Rev. B 7, 4388 (1973).

[30]M. Altarelli, W. Andreoni, and F. Bassani, Solid State Commun. 16, 143 (1975).

[31]See R. S. Knox, Ref. 1.

[32]G. F. Koster, J. O. Dimmock, R. G. Wheeler, and H. Statz, *Properties of the 32 point groups* (MIT, Cambridge, Mass., 1963).

[33]P. Rohner, Phys. Rev. B 3, 433 (1971).

[34]W. Andreoni and F. Casula (unpublished).